

A Selective and Sensitive Method for Colistin Detection by G-Quadruplex Ligand Competition

Shijiong Wei,[#] Dehui Qiu,[#] Xinrong Yan, Bin Liu, Jean-Louis Mergny, David Monchaud, Huangxian Ju,^{*} and Jun Zhou^{*}



Cite This: *Anal. Chem.* 2025, 97, 16805–16811



Read Online

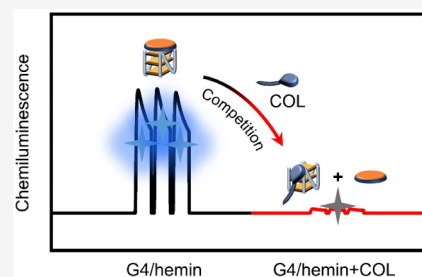
ACCESS |

Metrics & More

Article Recommendations

Supporting Information

ABSTRACT: Colistin (COL) is a widely used antibiotic and is quite often used as a last-resort treatment option for treating multidrug-resistant Gram-negative bacterial infections. Due to its widespread use, COL accumulates in nature, which represents a novel ecological and health threat. However, there is currently no rapid and specific method available for titrating COL levels in collected samples. Herein, we report a simple chemiluminescence detection method based on the specific interaction between COL and a parallel G-quadruplex (G4). To this end, we exploit the catalytic properties of the G4/hemin DNAzyme, which is able to oxidize substrates to provide a readily monitored readout. The stronger affinity of G4 for COL versus hemin allows for the inactivation of the G4/hemin DNAzyme, which is used herein to quantify COL in solution. Through a series of optimizations, we identified the best G4 sequence (F3TC), oxidation substrate (luminol), and experimental conditions, which allow for the detection of COL over a broad concentration window, from 0.5 to 2,500 ng/mL, with a detection limit of 0.4 ng/mL and excellent selectivity against other antibiotics. Compared with existing methods, the proposed approach provides a simpler and label-free quantification of COL, which might serve as a valuable standard method for antibiotic detection, whose use was validated under real conditions herein.



INTRODUCTION

Antimicrobial resistance has become a global health care crisis, as a growing number of pathogenic bacteria are resistant to currently available antimicrobial treatment.¹ Of particular concern are multidrug-resistant (MDR) Gram-negative bacteria (GNB). Colistin (COL, Figure 1A) has recently been reintroduced into clinical practice to treat infections caused by

MDR-GNB.^{2–4} First discovered in 1947, COL remained effective until resistance emerged in 2017. Despite this, COL retains good antimicrobial activity against many MDR-GNB stains, including certain carbapenem-resistant isolates.^{5,6} Furthermore, due to the stagnation of antibiotic development, COL is currently considered as a last-resort treatment option to combat the increasing prevalence of MDR-GNB.⁷ Unfortunately, COL has been misused in animal health, particularly as a growth promoter and for metaphylactic purposes.⁸ This misuse has contributed to the development of COL-resistant bacteria, posing significant risks to both animal and human health.⁹ COL has also been administered to entire groups of animals, including those without clinical symptoms, to prevent infections.¹⁰ This practice, common in pig farming, for instance, has contributed to the spread of colistin-resistant bacteria.¹¹

Growing evidence suggests that long-term exposure of bacteria to low COL concentrations may accelerate the spread of resistance genes, which, in turn, makes clinical treatment more difficult.¹² This is, for example, the case of *mobilized*

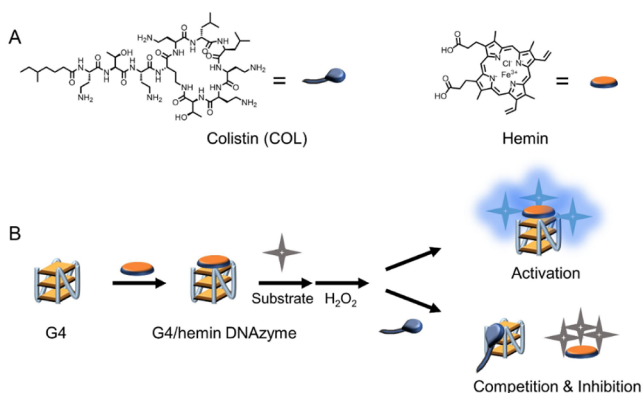


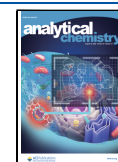
Figure 1. Schematic representation of the G4/hemin DNAzyme system for COL detection. (A) Structures of COL and hemin. (B) Substrate (luminol, NADH, and ABTS)–H₂O₂ system can be activated by the G4/hemin DNAzyme through the assembly of G4 and hemin, which can be inhibited by the competition from COL.

Received: March 23, 2025

Revised: July 11, 2025

Accepted: July 22, 2025

Published: July 31, 2025



colistin resistance (*MCR-1*) gene, which can be transferred between bacteria through plasmids. In humans, COL could be ingested with food (meat, dairy products)^{13,14} and cause organ damage or metabolic disorders.¹⁵ In addition, COL metabolites could be released into the environment through excrements (humans and animals), which can also contribute to both disrupt the balance of microbial communities and promote the spread of antibiotic resistance.^{16,17} Therefore, the detection of COL can ensure both health safety and environmental protection.

Considering that COL lacks aromatic amino acids (i.e., it does not exhibit exploitable UV–vis or fluorescence properties, Figures 1A and S1), detecting COL with high selectivity and sensitivity by traditional technologies is quite challenging.¹⁸ To quantify COL present in real samples, novel methods have been recently developed, including surface-enhanced Raman spectroscopy (SERS)¹⁹ and liquid chromatography coupled with mass spectrometry (LC-MS/MS).²⁰ Although efficient, these methods are tedious, notably for what concerns the sample preparation.¹⁸ Other techniques, such as the “sandwich immunoassay”,²¹ use anti-COL monoclonal antibodies and allow for a very selective COL detection, but their wide-scale implementation is limited mostly because of the cost of the antibodies.²² It is thus critical to propose a simple, universal, and robust method to detect COL.

We recently discovered that COL has an affinity for G-quadruplexes (G4s), especially for G4s with a parallel topology.²³ G4 is a four-stranded DNA structure formed by the stacking of G-tetrads (which are cyclic arrays of four guanines (Gs) held together by Hoogsteen-type hydrogen bonds).²⁴ Moreover, G4s are highly polymorphic and can be classified into three categories with parallel, antiparallel, and hybrid topologies.²⁵ Beyond the roles they may play in cellular biology,^{26,27} G4s are also privileged molecular tools to build biosensing devices. Notably, upon interaction with cofactors such as hemin, for instance, the resulting G4/hemin DNAzyme acquires a catalytic activity, enabling the oxidation of various organic substrates in a horseradish peroxidase (HRP)-like manner.^{28–30} Thanks to the programmability of G4 structures and the versatility of the resulting G4/hemin DNAzymes, this approach has been extensively used for biosensing applications, with the analyte being readily detected via chemiluminescence or photoelectric signals.^{31–33} In addition, G-quadruplex DNAzyme-based biocatalysis played an outstanding performance on antibiotics detection, such as tetracycline.³⁴

Herein, we proposed to implement this strategy to detect COL. To this end, the G4/hemin DNAzyme made from the G4-forming sequence F3TC, composed of d-[G₃TG₃TG₃TG₃TC], in interaction with hemin was used in the presence of H₂O₂ as a stoichiometric oxidant to detect COL in a simpler manner (Figure 1B). COL does indeed interfere with the F3TC/hemin catalytic properties as a result of competition for G4-binding between COL and hemin, the former having a higher G4 affinity than the latter. As further discussed below, a series of optimizations made to the G4-forming sequence, the substrate, and the experimental conditions have allowed for the chemiluminescence detection of COL (Figure 1B) in a range of 0.5 to 2,500 ng/mL and with a detection limit (LOD) of 0.4 ng/mL. Our method thus relies on a simple, inexpensive, and DNA-based system, whose efficiency surpasses most of the previously reported methods.

EXPERIMENTAL SECTION

Materials and Reagents. Colistin sulfate salt (COL), hemin, DMSO, tris(hydroxymethyl)-aminomethane (Tris), KCl, NaOH, thiazole orange (TO), Triton X-100, H₃BO₃, 2,2'-azino-bis(3-ethylbenzothiazoline 6-sulfonic acid) (ABTS), H₃PO₄, CH₃COOH, and TMAOH were purchased from Sigma-Aldrich (St. Louis, MO, USA). PAGE- or HPLC-purified DNA oligonucleotides, listed in Table S1, and luminol were sourced from Sangon Co., Ltd. (Shanghai, China). The Colistin ELISA Kit was purchased from Jiaozi Teng Co., Ltd. (Nanjing, China). All other chemical reagents were purchased from Aladdin (Shanghai, China). All reagents were of analytical grade and used without further purification.

Hemin was dissolved in DMSO to a final concentration of 100 μ M, and the mixture was stored in the dark at 4 °C. A 25 mM stock solution of luminol was prepared in a 0.1 M sodium hydroxide solution and stored at 4 °C. Working solutions of luminol were prepared by diluting the stock solution with ultrapure water. Fresh working solutions of H₂O₂ were prepared daily by the dilution of 30% (v/v) H₂O₂. A 1 mg/mL stock solution of COL was prepared using ultrapure water and stored at –20 °C. Gradient concentration COL solutions were prepared daily by the proper dilution of the stock solution.

Apparatus. UV–vis spectra were recorded using a Cary 3500 UV–vis spectrophotometer (Agilent Technologies, USA). Fluorescence (FL) spectra were measured by using a Cary Eclipse fluorescence spectrometer (Agilent Technologies, USA). Circular dichroism (CD) spectra were recorded on a Chirascan equipped with a Peltier temperature control accessory (Applied Photophysics, UK). Data from UV–vis, FL, and CD were collected with a 10 mm path length in a sealed tandem cuvette. Chemiluminescence detection was conducted on a MPI-A multifunctional electrochemical and chemiluminescent analytical system (Xi'an Remax Company, China) by adding H₂O₂ into a self-made cell with a MSP60–3A flow injection pump (Huiyu Weiye Beijing Fluid Equipment Co., Ltd., China). Biolayer interferometric (BLI) analyses were carried out using Octet K2 (Sartorius, Germany).

Preparation of G-Quadruplex Structure. Stock solutions of DNAs (200 μ M) in water were prepared in either 10 mM Tris-HCl buffer (pH 7) or 10 mM Britton–Robinson buffer (B–R, H₃BO₃/H₃PO₄/CH₃COOH/TMAOH, pH ranging from 6 to 9) with 100 mM KCl. To ensure the formation of G4 structures, the DNAs were denatured to 95 °C for 5 min and then slowly cooled to room temperature.

UV–Vis Absorption and Circular Dichroism (CD) Spectra. G4 samples were prepared in 10 mM Tris-HCl buffer (pH 7) containing 10 mM KCl and varying concentrations of COL. CD spectra were collected in the range of 220 to 350 nm, while UV–vis spectra were recorded from 220 to 800 nm.

Bio-Layer Interferometry (BLI). BLI analyses were performed using a BLItz system equipped with SA biosensors and conducted in BLItz binding buffer (10 mM Caco-LiOH, pH 7, 10 mM KCl, and 0.01% Tween). After immobilizing biotin-modified DNA oligonucleotides, association reactions were monitored at various concentrations of COL. The dissociation constant K_D and association constant K_a were calculated using default DataAnalysis 12 software.

Typical Oxidation Procedure. First, $0.4 \mu\text{M}$ G4s were incubated with $0.8 \mu\text{M}$ hemin at room temperature for 30 min. The reaction was initiated by adding $6 \mu\text{L}$ of 50 mM H_2O_2 and $6 \mu\text{L}$ of 50 mM ABTS. The generation of the oxidation product $\text{ABTS}^{\bullet+}$ was monitored by measuring the absorbance at 420 nm . The initial rate (V_0 , nM/s) of the oxidation reaction was determined from the slope of the initial linear portion (the first 10 s) of the absorbance vs reaction time plot. All kinetic measurements were performed in triplicate. All samples were prepared in 10 mM Tris-HCl buffer (pH 7) containing 0.05% (v/v) Triton X-100.

Measurement Procedure of COL. Ten μL of a mixture of G4s, diluted hemin, and luminol was incubated in 10 mM Tris-HCl buffer (pH 7) containing 10 mM KCl. Next, $30 \mu\text{L}$ of COL at different concentrations was added to the mixture. Finally, $200 \mu\text{L}$ H_2O_2 was injected into the cell at 1.33 mL/s using a MSP60–3A flow injection pump, and the chemiluminescence reaction was recorded.

Fluorescence Analysis of FAM-Labeled G-Quadruplex/Hemin with COL. $0.1 \mu\text{M}$ F3TC-FAM (F3TC labeled with FAM at the 3' terminus) was incubated in the presence or absence of hemin ($0.1 \mu\text{M}$) and then mixed with varying concentrations of COL (0 – $0.5 \mu\text{M}$) at room temperature for 30 min. FL spectra were measured from 500 to 650 nm , with excitation at 480 nm . All samples were prepared in 10 mM Tris-HCl (pH 7.0) containing 1% DMSO and 0.05% Triton X-100.

Selectivity Experiment and Recovery in Real Samples. Nine antibiotics, including streptomycin (STR), gentamicin (GEN), thiamphenicol (THI), chloramphenicol (CHL), fosfomicin (POS), and fluconazole (FLU), were chosen for selectivity experiments at concentrations of $12,500 \text{ ng/mL}$, while COL was used at 500 ng/mL . Milk and eggs were purchased from a local supermarket, and lake water was collected from Xiangxuehai Lake in the campus of Nanjing University. Milk samples were fortified with COL to final concentrations of 50 , 100 , and 500 ng/mL . Then, with the addition of an equal proportion of ethyl acetate, samples were mixed sufficiently and centrifuged at $3,000 \text{ rpm}$ for 20 min. The clear liquid in the tube was incubated with 0.1 mM H_2O_2 and dried at $45 \text{ }^\circ\text{C}$, followed by suspension in Tris-HCl buffer for further usage.³⁵ Egg and water samples were mixed with 20% trichloroacetic acid/acetonitrile and centrifuged at $5,000 \text{ rpm}$ for 5 min. The clear liquid was adjusted to pH 9 and purified by an SPE column. Detection procedures were performed according to the optimized conditions for COL detection. The recovery rate was determined as a ratio of the average concentration found in various samples to the fortified concentration.

RESULTS AND DISCUSSION

G4 Topology Regulates Inhibition of Catalysis on G4/Hemin DNAzyme. We previously showed that COL can specifically bind to parallel G4.²³ Further circular dichroism (CD)³⁶ and UV–vis data confirmed this conclusion (Figure S2). We thus investigated the catalytic properties of G4/hemin DNAzymes in the presence of COL: using ABTS as a chromogenic substrate and H_2O_2 as an oxidant, we studied the catalytic efficiency of several G4/hemin DNAzymes, quantified by the initial velocity (V_0 , nM/s) of the oxidation reaction, assessed by the measurement of absorbance of $\text{ABTS}^{\bullet+}$ at 420 nm as a function of time. As seen in Figure 2A, the parallel G4 N-myc ($V_0 = 178 \text{ nM/s}$) has better performance than the

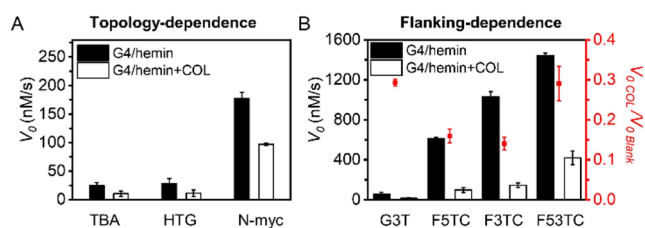


Figure 2. COL inhibits the catalytic activity on the G4/hemin DNAzyme. (A) Topology- and (B) flanking-dependence inhibition on the catalytic activity of H_2O_2 -promoted oxidation catalyzed by the G4/hemin DNAzyme in the absence and presence of $5 \mu\text{g/mL}$ COL, as accessed by the initial rate V_0 . The raw data are provided in Figures S3 and S4. The G4 sequences, TBA, HTG, and N-myc, are antiparallel, hybrid, and parallel G4, respectively. All the sequences used in this experiment are listed in Table S1.

antiparallel G4 TBA ($V_0 = 24.7 \text{ nM/s}$) and the hybrid G4 HTG ($V_0 = 28.5 \text{ nM/s}$) (Table S2). This probably originates from better accessibility of the terminal tetrads in parallel G4s, in which loops are located in the grooves,²⁵ facilitating interaction with hemin (which π -stacks atop the external G-quartet of the G4).^{37,38} Interestingly, the catalytic capacity of the G4/hemin DNAzyme was substantially inhibited with the addition of COL (Figure S3): the difference in initial velocity, ΔV_0 ($V_{0 \text{ blank}} - V_{0 \text{ COL}}$), is higher with the parallel G4 N-myc ($\Delta V_0 = 80.7 \text{ nM/s}$, -44.6%) than nonparallel G4s TBA and HTG ($\Delta V_0 = 17.3 \text{ nM/s}$, -39.3%) and TBA ($\Delta V_0 = 14.1 \text{ nM/s}$, -42.9%) (Figure 2A and Table S2).

Flanking Regulates Inhibition of Catalysis on G4/Hemin DNAzyme. In order to optimize the difference in COL inhibition properties, we studied the effect of flanking d[TC] added to the parallel G4 structure. CD and UV–vis analyses indicated that the addition of d[TC] at the terminal ends of G3T did not alter its parallel topology of parallel G4 (Figure S5). However, the presence of COL triggers different effects as it significantly changes both the ellipticity and absorbance of d[TC]-flanked G4s, notably F53TC d-[CTG₃TG₃TG₃TC], with d[TC] at both 5' and 3' terminals, suggesting that the flanking sequences of parallel G4s can enhance COL binding. Next, we employed the ABTS– H_2O_2 system as above to investigate the inhibition of COL in the presence of an additional d[TC] flanking sequence. As previously reported,³⁰ the addition of d[TC] significantly enhances the catalytic properties of the resulting G4/hemin DNAzyme, especially for F53TC ($V_0 = 1445 \text{ nM/s}$), exhibiting d[TC] flanking sequences at both 5' and 3' ends (Figure S4). Upon addition of COL, the catalytic efficiency was inhibited for all G4s, without (i.e., G3T, $V_{0 \text{ COL}}/V_{0 \text{ blank}} = 0.296$) or with flanking sequence, on the 3' end (F3TC, $V_{0 \text{ COL}}/V_{0 \text{ blank}} = 0.141$) or on the 5' end (F5TC, $V_{0 \text{ COL}}/V_{0 \text{ blank}} = 0.160$), or both (F53TC, $V_{0 \text{ COL}}/V_{0 \text{ blank}} = 0.291$) (Figures 2B and S4). Both the higher initial activity of F3TC ($V_0 = 1033 \text{ nM/s}$) and the higher COL-mediated inhibition observed with F3TC make it ideally suited to further experiments (Table S2).

Binding Mechanism between COL and G4/Hemin DNAzyme. To go one step further, the G4/COL binding mechanism was studied by biolayer interferometry (BLI) experiments. The dissociation equilibrium constant (K_D) and association constant (K_A) of COL for F3TC were found to be 18.1 nM and $5.52 \times 10^7 \text{ M}^{-1}$, respectively, which are far lower than those of hemin ($1.89 \mu\text{M}$ and $5.29 \times 10^5 \text{ M}^{-1}$,

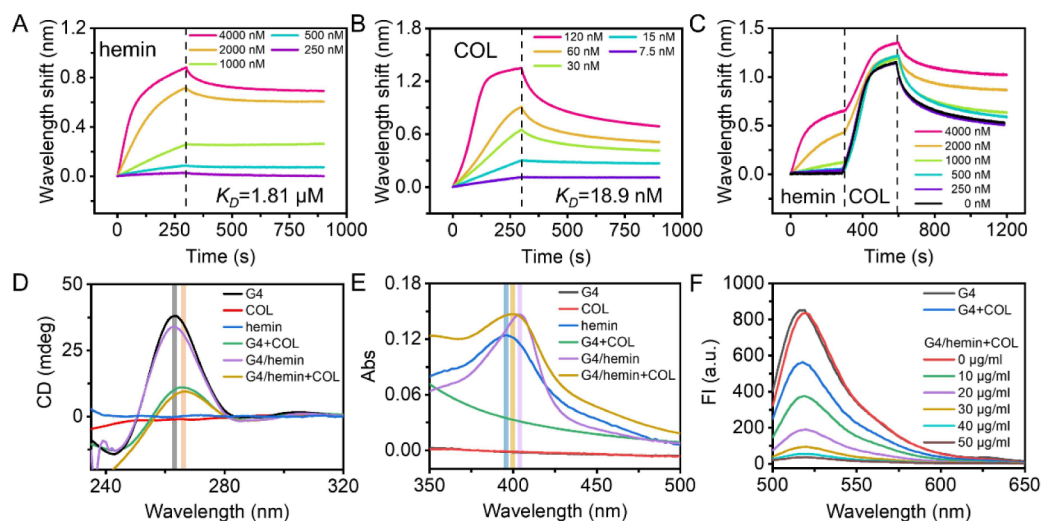


Figure 3. COL competes with hemin for G4 binding. Bio-Layer Interferometry (BLI) binding kinetics of (A) hemin and (B) COL toward F3TC G4. The concentration of hemin ranges from 250 to 4000 nM and COL from 7.5 to 120 nM. (C) Competitive binding between hemin and COL toward G4. The concentration of COL is 120 nM, while that of hemin ranges from 0 to 4000 nM. (D) CD and (E) UV–vis spectra of 5 μ M G4, 10 μ M COL, 10 μ M hemin, and G4/hemin in the absence and presence of 10 μ M COL. Marked lines in gray (263 nm) and yellow (266 nm) in (D) are the specific peaks of G4 in the absence and presence of COL, respectively; and marked lines in blue (394 nm), purple (404 nm), and yellow (400 nm) in (E) are specific absorbance of hemin, G4/hemin in the absence and presence of COL, respectively. (F) Normalized fluorescence emission spectra (excitation at 480 nm) of F3TC-FAM (0.1 μ M DNA) with hemin (0.1 μ M) in the presence of varying COL and without hemin in the presence of 0.1 μ M COL.

respectively), indicating that the G4/COL interaction is stronger than that of G4/hemin (Figure 3A,B). This was further studied by fluorescent intercalator displacement (FID) performed with NMM, which binds to the G-quartet of a G4,³⁹ Hoechst 33258, which tends to bind to the G4 grooves,³⁹ and TO, which binds to both the G-quartet and grooves.^{40,41} The fluorescence of these G4 ligands was first turned on upon interaction with G4s and then progressively decreased upon the addition of increasing amounts of COL in all instances, suggesting that COL can bind to G4 in two ways (Figure S6).²³ COL can thus occupy the binding site of hemin: this was verified by four different experiments, i.e., competitive BLI, CD, UV–vis, and fluorescence experiments. As seen in Figure 3C, when COL is added to 4 μ M of a preformed G4/hemin complex, a significant wavelength shift is observed, even for low concentrations of COL, down to 120 nM, indicating that COL effectively competes with hemin for binding to the G4/hemin complex.

Competed interaction was confirmed by CD titrations: as seen in Figure 3D, while hemin had no impact on the G4 topology, COL could decrease the CD signal (ellipticity) corresponding to the G4; when hemin was added first, COL could still induce a decrease in G4 ellipticity, indicating that COL efficiently competes with hemin for G4 binding. As seen in Figures 3E and S1, COL does not have specific spectral features in the UV–vis region, while hemin exhibited an absorption peak around 394 nm; its interaction with G4s triggers a hyperchromic shift at 404 nm (which is often used to testify for the formation of G4/hemin DNAses).²⁹ Upon addition of COL to a preformed G4/hemin complex, a hypsochromic shift at 400 nm is observed, indicating that COL disrupts the G4/hemin binding, which in turn could lead to the inhibition of its G4/hemin DNase activity. Finally, as seen in Figure 3F, fluorescence titrations can also be used to confirm this competition: the fluorescence of a preformed G4/hemin complex gradually decreased with increasing amounts of

COL, indicating that hemin cannot prevent the binding of COL to G4. Taken together, these results suggest that COL disrupts the stacking of hemin onto G4, which therefore could inhibit the catalytic activity of the corresponding G4/hemin DNase, likely because of the higher G4 affinity of COL versus hemin.

Optimization of COL Detection. To further identify the best system for COL detection, we next evaluated three substrates, i.e., NADH, ABTS, and luminol, with a G4/hemin system made with F3TC. As shown in Figure S7, using luminol led to the highest decrease in chemiluminescent intensity at 425 nm upon COL addition; the two other substrates, NADH and ABTS, lead to moderate responses only (from 0.2 to 0.8 mg/mL for NADH; from 1 to 5 μ g/mL for ABTS, Figures S4 and S8). Of note, ABTS offers the possibility of implementing a colorimetric analysis of COL: as seen in Figure S9, this approach turned out to be efficient for a concentration range of 2.5 to 20 μ M. We further investigated the use of luminol: as seen in Figures 4 and S10, its oxidation using different G4/hemin DNAses is significantly affected when G4 is F3TC (86.8%) versus G3T (71.7%) and N-myc (43.2%). We

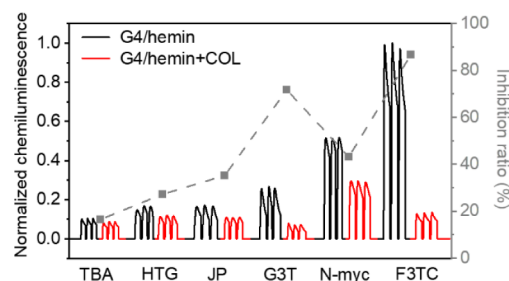


Figure 4. Sequence dependence of inhibition on the catalytic activity of H_2O_2 -promoted oxidation of luminol catalyzed by the G4/hemin DNase system in the absence (black) and presence (red) of 10 μ g/mL COL.

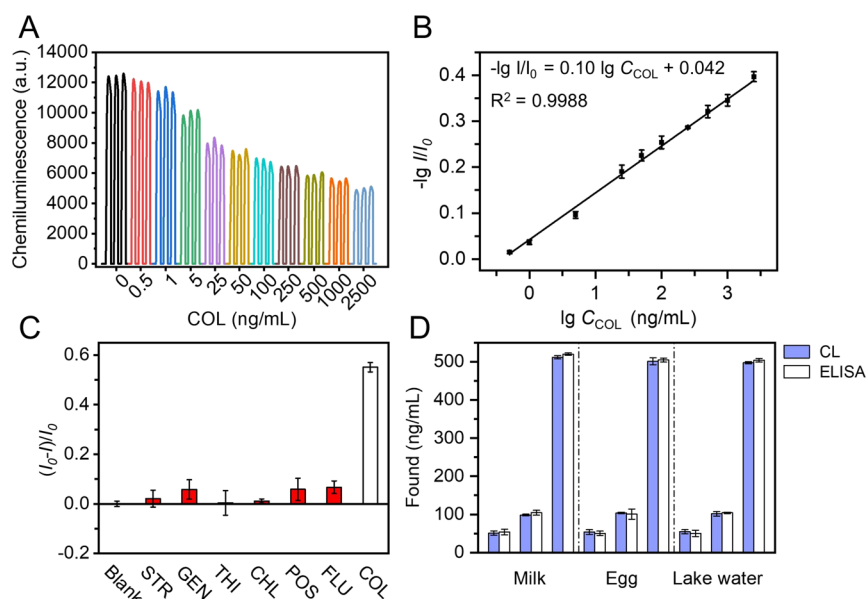


Figure 5. F3TC/hemin DNzyme system for COL detection, selectivity experiments, and recovery tests. (A) Chemiluminescence spectra of the F3TC/hemin–luminol– H_2O_2 system with different concentrations of COL. (B) Linear relationship between the logarithm of the inhibition ratio of chemiluminescence intensity (I/I_0) and the logarithm of COL concentration, ranging from 0.5 to 2500 ng/mL. (C) Effect of various antibiotics on the chemiluminescence intensity of the F3TC/hemin–luminol– H_2O_2 system. The concentrations of COL and other antibiotics were 500 ng/mL and 12500 ng/mL, respectively. STR, GEN, THI, CHL, POS, FLU, and COL correspond to streptomycin, gentamicin, thiamphenicol, chloramphenicol, fluconazole, and colistin, respectively. I_0 and I represent the chemiluminescence intensity in the absence and presence of antibiotics, respectively; the other conditions are the same as those in Figure S12. (D) Spiked COL in milk, eggs, and lake water, which were determined by the F3TC/hemin–luminol– H_2O_2 system, and the chemiluminescence (CL) results were compared with those obtained using ELISA.

assumed that the best inhibition of the G4/hemin system observed in F3TC may result from its better catalytic activity with hemin (Figure 2B) and COL prefers parallel G4s with flanks (Figure S5). We thus used this system for further optimizations.

To assess the COL detection sensitivity using chemiluminescence, we first investigated the ion effect and found that common ions, such as K^+ , Na^+ and Ca^{2+} , did not affect the inhibition of G4/hemin DNzyme with the addition of COL (Figure S11). Then, we optimized the experimental conditions by modifying the pH of the solution and the concentrations of the reaction partners (luminol, hemin, F3TC, and H_2O_2). The optimal catalytic activity of G4/hemin DNzyme was found to be in a slightly acidic medium,³⁰ while the chemiluminescence of luminol was optimized in an alkaline medium.⁴² We therefore investigated the effect of pH in the range of 6.0 to 9.0 and found that the optimum pH was 7.0 (Figure S12A). The optimal concentrations of luminol, hemin, F3TC, and H_2O_2 were determined to be 1.7 μM , 0.25 nM, 1.0 nM, and 7.5 mM, respectively (Figure S12B–E). Lastly, the optimal incubation time was determined to be 1 min based on the optimized experiments (Figure S12F).

Detection of COL Based on F3TC/Hemin DNzyme.

These optimized conditions were thus used to detect various concentrations of COL. As seen in Figure 5A, the addition of COL can remarkably inhibit chemiluminescence. The profiles of the titration indicated that increasing concentrations of COL trigger a decrease of the COL emission intensity in a linear manner (with a remarkable correlation coefficient of 0.9988) in the range of COL concentrations from 0.5 to 2500 ng/mL (Figure 5B). The detection limit was calculated to be 0.4 ng/mL (by a signal-to-noise ratio of 3), which is 125-fold lower than the maximum residue limit (50 ng/mL) in milk, as

recommended by the European Union.⁸ This novel system turned out to be competitive with the best system reported so far (Table S3), being however far less expensive than the antibodies (ELISA) or the high-tech machines (SERS) used in competitive technologies. To evaluate the selectivity and reliability of this new method, several common antibiotics, i.e., STR, GEN, THI, CHL, POS, and FLU (Figure S13), were tested at a concentration of 12.5 mg/mL, i.e., 25-fold higher than that of COL (500 ng/mL): as seen in Figure 5C, the $(I - I_0)/I_0$ signal for COL was ca. 8-fold higher than that obtained with other antibiotics, confirming the excellent selectivity of this system for COL versus other antibiotics. Finally, we investigated whether it might be efficient in real conditions: to this end, real samples were supplemented with 50, 100, and 500 ng/mL of COL; as seen in Figure 5D, compared with ELISA, our method displayed similar performance in recovery, thus confirming its reliability.

CONCLUSION

In this work, we first establish a novel chemiluminescence-based system involving a G4 unit (F3TC), a cofactor (hemin) to assemble a G4/hemin DNzyme usable for the specific and sensitive detection of COL, on the basis of a competition for G4-binding between COL and hemin. We optimized the catalytic conditions (concentrations, pH, etc.) and selected the best substrate (luminol) to provide a system able to detect COL with a limit as low as 0.4 ng/mL, without the need for expensive molecular tools (e.g., antibodies) or instruments (e.g., Raman spectrometer). Altogether, this work addresses a gap in COL detection and provides an easy-to-implement method that has proven to be very effective under real conditions.

■ ASSOCIATED CONTENT

SI Supporting Information

The Supporting Information is available free of charge at <https://pubs.acs.org/doi/10.1021/acs.analchem.5c01733>.

Materials and methods; interaction of G4 and COL analyzed by UV–vis, CD, and fluorescence; plots of absorbance at 350 and 420 nm as a function the time; colorimetric analysis; comparison of oxidation substrates; and statistical analysis and Figures S1–S13 and Tables S1–S3 (PDF)

■ AUTHOR INFORMATION

Corresponding Authors

Huangxian Ju – State Key Laboratory of Analytical Chemistry for Life Science, School of Chemistry and Chemical Engineering, Nanjing University, Nanjing 210093, P.R. China; orcid.org/0000-0002-6741-5302; Email: hxju@nju.edu.cn

Jun Zhou – State Key Laboratory of Analytical Chemistry for Life Science, School of Chemistry and Chemical Engineering, Nanjing University, Nanjing 210093, P.R. China; orcid.org/0000-0002-6793-3169; Email: jun.zhou@nju.edu.cn

Authors

Shijiong Wei – State Key Laboratory of Analytical Chemistry for Life Science, School of Chemistry and Chemical Engineering, Nanjing University, Nanjing 210093, P.R. China

Dehui Qiu – State Key Laboratory of Analytical Chemistry for Life Science, School of Chemistry and Chemical Engineering, Nanjing University, Nanjing 210093, P.R. China

Xinrong Yan – State Key Laboratory of Analytical Chemistry for Life Science, School of Chemistry and Chemical Engineering, Nanjing University, Nanjing 210093, P.R. China; orcid.org/0009-0003-5574-2546

Bin Liu – State Key Laboratory of Analytical Chemistry for Life Science, School of Chemistry and Chemical Engineering, Nanjing University, Nanjing 210093, P.R. China

Jean-Louis Mergny – State Key Laboratory of Analytical Chemistry for Life Science, School of Chemistry and Chemical Engineering, Nanjing University, Nanjing 210093, P.R. China; Laboratoire d'Optique et Biosciences (LOB), Ecole Polytechnique, CNRS, INSERM, Institut Polytechnique de Paris, Palaiseau 91120, France; orcid.org/0000-0003-3043-8401

David Monchaud – Institut de Chimie Moléculaire de l'Université de Bourgogne (ICMUB), CNRS UMR6302, Université Bourgogne Europe (UBE), Dijon 21078, France; orcid.org/0000-0002-3056-9295

Complete contact information is available at: <https://pubs.acs.org/doi/10.1021/acs.analchem.5c01733>

Author Contributions

[#]S.W. and D.Q. contributed equally to this paper.

Notes

The authors declare no competing financial interest.

■ ACKNOWLEDGMENTS

We gratefully acknowledge the National Natural Science Foundation of China (22177047, 22374070), the State Key Laboratory of Analytical Chemistry for Life Science

(5431ZZXM2406), and the Fundamental Research Funds for the Central Universities (202200324, 202200325, and 020514380299). J.L.M. acknowledges support from Fondation de l'École Polytechnique.

■ REFERENCES

- (1) Blair, J. M. A.; Webber, M. A.; Baylay, A. J.; Ogbolu, D. O.; Piddock, L. J. V. *Nat. Rev. Microbiol.* **2015**, *13* (1), 42–51.
- (2) Li, J.; Nation, R. L.; Turnidge, J. D.; Milne, R. W.; Coulthard, K.; Rayner, C. R.; Paterson, D. L. *Lancet Infect. Dis.* **2006**, *6* (9), 589–601.
- (3) Bergen, P. J.; Landersdorfer, C. B.; Zhang, J.; Zhao, M.; Lee, H. J.; Nation, R. L.; Li, J. *Diagn. Microbiol. Infect. Dis.* **2012**, *74* (3), 213–223.
- (4) Nation, R. L.; Li, J. *Curr. Opin. Infect. Dis.* **2009**, *22* (6), 535–543.
- (5) Sabnis, A.; Hagart, K. L. H.; Klöckner, A.; Becce, M.; Evans, L. E.; Furniss, R. C. D.; Mavridou, D. A. I.; Murphy, R.; Stevens, M. M.; Davies, J. C.; et al. *eLife* **2021**, *10*, No. e65836.
- (6) Yahav, D.; Farbman, L.; Leibovici, L.; Paul, M. *Clin. Microbiol. Infect.* **2012**, *18* (1), 18–29.
- (7) Rúbies, A.; Beguiristain, I.; Tibon, J.; Cortés-Francisco, N.; Granados, M. *Food Chem.* **2024**, *443*, 138481.
- (8) Kumar, H.; Chen, B.-H.; Kuca, K.; Nepovimova, E.; Kaushal, A.; Nagraik, R.; Bhatia, S. K.; Dhanjal, D. S.; Kumar, V.; Kumar, A.; Upadhyay, N. K.; Verma, R.; Kumar, D. *Animals* **2020**, *10* (10), 1892.
- (9) MacNair, C. R.; Stokes, J. M.; Carfrae, L. A.; Fiebig-Comyn, A. A.; Coombes, B. K.; Mulvey, M. R.; Brown, E. D. *Nat. Commun.* **2018**, *9* (1), 458.
- (10) Hernández, M.; Iglesias, M. R.; Rodríguez-Lázaro, D.; Gallardo, A.; Quijada, N.; Miguela-Villoldo, P.; Campos, M. J.; Píriz, S.; López-Orozco, G.; de Frutos, C.; et al. *Eurosurveillance* **2015**, *22* (31), 30586.
- (11) Peng, Z.; Hu, Z.; Li, Z.; Zhang, X.; Jia, C.; Li, T.; Dai, M.; Tan, C.; Xu, Z.; Wu, B.; et al. *Nat. Commun.* **2022**, *13* (1), 1116.
- (12) Qiu, S.; Liu, K.; Yang, C.; Xiang, Y.; Min, K.; Zhu, K.; Liu, H.; Du, X.; Yang, M.; Wang, L.; et al. *Nat. Commun.* **2022**, *13* (1), 7365.
- (13) Gai, Z.; Samodelov, S. L.; Kullak-Ublick, G. A.; Visentin, M. *Molecules* **2019**, *24* (3), 653.
- (14) Velkov, T.; Dai, C.; Ciccotosto, G. D.; Cappai, R.; Hoyer, D.; Li, J. *Pharmacol. Ther.* **2018**, *181*, 85–90.
- (15) Rhouma, M.; Beaudry, F.; Thériault, W.; Letellier, A. *Front. Microbiol.* **2016**, *7*, 1789.
- (16) Sanderson, H.; Fricker, C.; Brown, R. S.; Majury, A.; Liss, S. N. *Environ. Rev.* **2016**, *24* (2), 205–218.
- (17) Xie, M.; Zhang, Y.; Chen, K.; Dong, N.; Zhou, H.; Huang, Y.; Liu, C.; Chan, E. W.-C.; Chen, S.; Zhang, R. *Commun. Med.* **2025**, *5* (1), 73.
- (18) Galvidis, I. A.; Eremin, S. A.; Burkin, M. A. *Food Agric. Immunol.* **2020**, *31* (1), 424–434.
- (19) Li, Y.; Tang, S.; Zhang, W.; Cui, X.; Zhang, Y.; Jin, Y.; Zhang, X.; Chen, Y. *Sens. Actuators, B* **2019**, *282*, 703–711.
- (20) Boison, J. O.; Lee, S.; Matus, J. *Anal. Bioanal. Chem.* **2015**, *407* (14), 4065–4078.
- (21) Xu, L.; Burkin, M.; Eremin, S.; Dias, A. C. P.; Zhang, X. *Food Anal. Methods* **2019**, *12* (6), 1412–1419.
- (22) Sarawagi, N.; Vaid, K.; Dhiman, J.; Johns, T.; Kumar, V. Nanomaterials-based immunosensors in food analysis. In *Nanosensing and Bioanalytical Technologies in Food Quality Control*, Chandra, P.; Panesar, P. S., Eds.; Singapore: Springer Singapore, 2022; pp. 259–318.
- (23) Wei, S.; Zhang, X.; Feng, Y.; Tao, S.; Qiu, D.; Yan, X.; Li, G.; Guittat, L.; Zhang, W.; Monchaud, D.; Mergny, J.-L.; Ju, H.; Zhou, J. *J. Am. Chem. Soc.* **2025**, *147* (11), 9962–9971.
- (24) Mergny, J.-L.; Sen, D. *Chem. Rev.* **2019**, *119* (10), 6290–6325.
- (25) Burge, S.; Parkinson, G. N.; Hazel, P.; Todd, A. K.; Neidle, S. *Nucleic Acids Res.* **2006**, *34* (19), 5402–5415.

- (26) Varshney, D.; Spiegel, J.; Zyner, K.; Tannahill, D.; Balasubramanian, S. *Nat. Rev. Mol. Cell Biol.* **2020**, *21* (8), 459–474.
- (27) Esnault, C.; Magat, T.; Zine El Aabidine, A.; Garcia-Oliver, E.; Cucchiaroni, A.; Bouchouika, S.; Lleres, D.; Goerke, L.; Luo, Y.; Verga, D.; Lacroix, L.; Feil, R.; Spicuglia, S.; Mergny, J.-L.; Andrau, J.-C. *Nat. Genet.* **2023**, *55* (8), 1359–1369.
- (28) Cheng, Y.; Cheng, M.; Hao, J.; Jia, G.; Monchaud, D.; Li, C. *Chem. Sci.* **2020**, *11* (33), 8846–8853.
- (29) Qiu, D.; Cheng, M.; Stadlbauer, P.; Chen, J.; Langer, M.; Zhang, X.; Gao, Q.; Ju, H.; Sponer, J.; Mergny, J.-L.; Monchaud, D.; Zhou, J. *ACS Catal.* **2023**, *13* (16), 10722–10733.
- (30) Chen, J.; Zhang, Y.; Cheng, M.; Guo, Y.; Sponer, J.; Monchaud, D.; Mergny, J.-L.; Ju, H.; Zhou, J. *ACS Catal.* **2018**, *8* (12), 11352–11361.
- (31) Mao, X.; He, F.; Qiu, D.; Wei, S.; Luo, R.; Chen, Y.; Zhang, X.; Lei, J.; Monchaud, D.; Mergny, J.-L.; Ju, H.; Zhou, J. *Anal. Chem.* **2022**, *94* (20), 7295–7302.
- (32) Liu, B.; Wang, T.; Qiu, D.; Yan, X.; Liu, Y.; Mergny, J.-L.; Zhang, X.; Monchaud, D.; Ju, H.; Zhou, J. *Anal. Chem.* **2024**, *96* (36), 14590–14597.
- (33) Ge, R.; Zhang, S.; Dai, H.; Wei, J.; Jiao, T.; Chen, Q.; Chen, Q.; Chen, X. *J. Agric. Food Chem.* **2023**, *71* (44), 16807–16814.
- (34) Wang, L.; Wang, W.; Zhang, S.; Wei, J.; Chen, Q.; Jiao, T.; Lin, A.; Chen, Q.; Chen, X. *J. Agric. Food Chem.* **2025**, *73* (2), 1598–1607.
- (35) Song, E.; Yu, M.; Wang, Y.; Hu, W.; Cheng, D.; Swihart, M. T.; Song, Y. *Biosens. Bioelectron.* **2015**, *72*, 320–325.
- (36) Kyrp, J.; Kejnovska, I.; Renciuik, D.; Vorlickova, M. *Nucleic Acids Res.* **2009**, *37* (6), 1713–1725.
- (37) Kong, D.-M.; Yang, W.; Wu, J.; Li, C.-X.; Shen, H.-X. *Analyst* **2010**, *135* (2), 321–326.
- (38) Cheng, X.; Liu, X.; Bing, T.; Cao, Z.; Shangguan, D. *Biochemistry* **2009**, *48* (33), 7817–7823.
- (39) Monchaud, D.; Teulade-Fichou, M. P. *Org. Biomol. Chem* **2008**, *6* (4), 627–636.
- (40) Vummidi, B. R.; Alzeer, J.; Luedtke, N. W. *ChemBiochem* **2013**, *14* (5), 540–558.
- (41) Guo, R.-J.; Yan, J.-W.; Chen, S.-B.; Gu, L.-Q.; Huang, Z.-S.; Tan, J.-H. *Dyes Pigm.* **2016**, *126*, 76–85.
- (42) Haapakka, K. E.; Kankare, J. J. *Anal. Chim. Acta* **1982**, *138*, 263–275.



CAS BIOFINDER DISCOVERY PLATFORM™

ELIMINATE DATA SILOS. FIND WHAT YOU NEED, WHEN YOU NEED IT.

A single platform for relevant, high-quality biological and toxicology research

Streamline your R&D

CAS
A division of the American Chemical Society